Search for candidate chiral nuclei in rubidium isotopes

B. Qi (亓斌),* H. Jia (贾慧), C. Liu (刘晨), and S. Y. Wang (王守宇)†

Shandong Provincial Key Laboratory of Optical Astronomy and Solar-Terrestrial Environment, School of Space Science and Physics, Institute of Space Sciences, Shandong University, Weihai 264209, People's Republic of China

(Received 12 April 2018; revised manuscript received 31 May 2018; published 5 July 2018)

The chirality in rubidium isotopes is investigated for the first time by using adiabatic and configuration-fixed constrained triaxial relativistic mean-field theory. Several minima with the triaxial deformation and proper particle-hole configuration are obtained in ^{78,80,82,86}Rb where the chiral doublet bands are possible to appear. Furthermore, the possible existence of multiple chiral doublet (MχD) bands is demonstrated in ^{78,80,82}Rb. The experimental explorations for the chirality and MχD in Rb isotopes are expected to verify the predictions.

DOI: 10.1103/PhysRevC.98.014305

I. INTRODUCTION

Chiral symmetry breaking in atomic nuclei has attracted extensive discussions since it was predicted by Frauendorf and Meng [1]. They pointed out that, in the intrinsic frame of the rotating triaxial nucleus with a few high-j valence particles and a few high-j valence holes, the total angular momentum vector may lie outside the three principal planes, referred to as chiral geometry. Due to the chiral symmetry breaking, a pair of nearly degenerate $\Delta I = 1$ bands with the same parity, i.e., chiral doublet bands, should be observed in the laboratory frame. Such chiral doublet bands were first observed in the $N = 75$ isotones [2]. So far, more than 40 experimental candidates have been reported in the $A \sim 80$, 100, 130, and 190 mass regions, see, e.g., Refs. [2–25]. Theoretically, chiral doublet bands have been described successfully in many models [26–47]. An overview of these studies and open problems in understanding the nuclear chirality is introduced in Ref. [48].

Based on constrained triaxial relativistic mean-field (RMF) theory calculations, it has been suggested that multiple chiral doublet (MχD) bands can exist in a single nucleus [49]. The theoretical prediction of MχD bands stimulated lots of experimental efforts. The first experimental evidence for MχD bands was reported in ^{133}Ce [22], which confirmed the manifestation of triaxial shape coexistence in this nucleus. Later, a novel type of MχD band with the same configuration was reported in ^{103}Rh [23], which showed that chiral geometry can be robust against the increase in the intrinsic excitation energy.

This paper focuses on the chirality in the 80-mass region. In 2011, a pair of positive-parity doublet bands with the $\pi g_{9/2} \otimes \nu g_{9/2}^{-1}$ configuration in ^{80}Br was reported as the first evidence of the chiral doublet bands in the $A \sim 80$ region [24]. In 2016, two pairs of positive- and negative-parity doublet bands have been identified in ^{78}Br, which are interpreted as MχD with octupole correlations [25]. The configurations are corresponding to $\pi g_{9/2} \otimes \nu g_{9/2}^{-1}$ and $\pi(f_{5/2}/p_{3/2}) \otimes \nu g_{9/2}^{-1}$, respectively.

It is interesting to explore whether or not chirality and MχD exist in the other isotopes of the $A \sim 80$ mass region except the Br isotopes ($Z = 35$). By investigating the available experimental data of the neighboring rubidium isotopes ($Z = 37$), namely, $^{76-86}$Rb [50–60], it is found that the chirality in the Rb isotopes was not reported and discussed so far. However, we note that a pair of positive-parity doublet bands (labeled 1 and 2) with the assigned $\pi g_{9/2} \otimes \nu g_{9/2}$ configuration in ^{78}Rb [52] and a pair of negative-parity doublet bands with the assigned $\pi f_{5/2} \otimes \nu g_{9/2}$ configuration in ^{80}Rb [53] show the characteristic of chiral doublet bands, i.e., nearly degenerate $\Delta I = 1$ bands.

Motivated by the above considerations, we adopt the adiabatic and configuration-fixed constrained triaxial RMF theory to study the deformations and the corresponding configurations in the Rb isotopes and to explore whether or not chirality and MχD exist in these nuclei.

II. DISCUSSION

The starting point of the RMF theory is the standard effective Lagrangian density constructed with the degrees of freedom associated with the nucleon field, σ, ω, and ρ meson fields, and the photon field. This theory has successfully described the triaxial shape coexistence and possible MχD in many nuclei, e.g., ^{104,106,108,110}Rh [49,61,62], ^{103,105}Rh [23,63], ^{107}Ag [64], ^{125,129,131}Cs [65], and ^{133}Ce [22]. The details of the formalism and numerical techniques of the triaxial RMF can be seen in Ref. [61]. In the present triaxial RMF calculations, the time-odd fields are included. We employ a spherical harmonic-oscillator basis with 12 major shells for fermions and 10 shells for bosons. Due to the Pauli block effect, pairing correlations in the odd-odd nuclei are neglected.

The calculated results with parameter set PK1 [66] are shown in this paper, and it has been verified that a very similar conclusion could be obtained adopting the NL3 [67] or TM1 [68] parameter sets. The constrained calculations with $\langle \hat{Q}_{20}^2 + 2\hat{Q}_{22}^2 \rangle$, i.e., β^2, are carried out to search for the ground state for

*bqi@sdu.edu.cn
†sywang@sdu.edu.cn

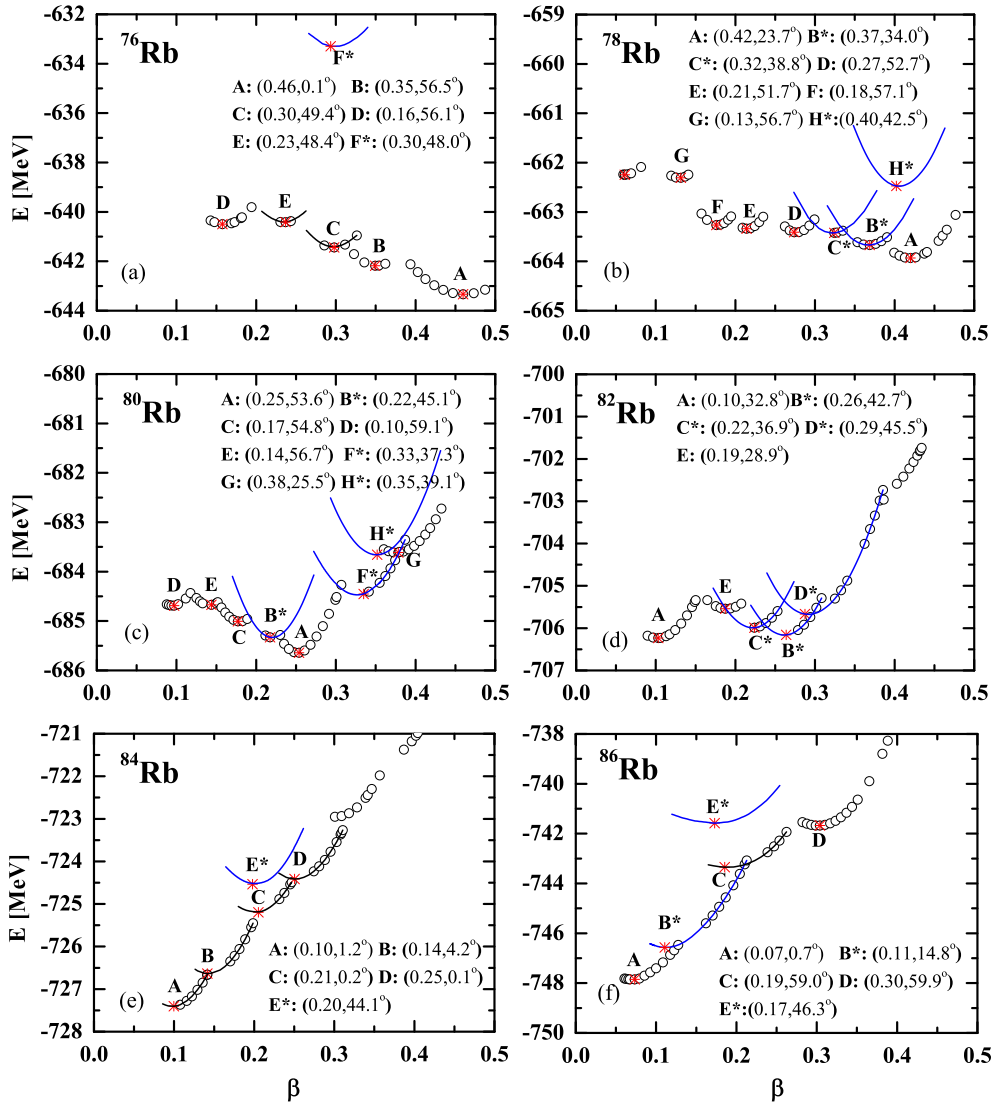

FIG. 1. The energy surfaces in the adiabatic (open circles) and configuration-fixed (solid lines) constrained triaxial RMF calculations with PK1 for ^{76,78,80,82,84,86}Rb. The minima in the energy surfaces for the fixed configuration are represented as stars and are labeled as A, B, C, D, E, F, G, and H, respectively. Their corresponding triaxial deformation parameters β and γ are also given. The suitable states for the appearance of the chirality are marked by the blue color and asterisks.

a triaxially deformed nucleus here. During the β-constrained calculations, triaxial deformation is automatically obtained by minimizing the energy. First, the adiabatic constrained calculation is used to obtain the states with different configurations, and then the configuration-fixed constrained calculation is performed. Here the adiabatic constrained calculation means that the nucleons always occupy the lowest single-particle levels, whereas the configuration-fixed constrained calculation means that the nucleons must occupy the same combination of the single-particle levels during the constraint process [49,62].

The calculated energy surfaces in ^{76,78,80,82,84,86}Rb, based on adiabatic and configuration-fixed constrained triaxial RMF theory, are presented in Fig. 1. The minima in the energy surfaces for the fixed configuration are represented as stars and labeled as A, B, C, D, E, F, G, and H, respectively. The triaxiality parameter γ obtained by minimizing the energy is given as a function of β in Fig. 2. The shaded areas in the figures represent the triaxiality parameter γ, favorable for nuclear chirality.

As the triaxial deformation is the necessary condition for the nuclear chirality, thus we first search for the minima of the triaxial deformation. As shown in Figs. 1 and 2, ^{78,80,82}Rb have more than one minimum state with triaxial deformations, which provide good examples of triaxial shape coexistence. Meanwhile, for adiabatic calculations, only one triaxial local minimum (state B) is obtained in ^{86}Rb, and no triaxial minimum is found in ^{76}Rb and ^{84}Rb. For ^{76}Rb and ^{84}Rb, if we perform the particle-hole excitation to achieve the $\pi g_{9/2} \otimes \nu g_{9/2}^{-1}$ configuration, the triaxial minima may occur. However, the excited energies of these states are too high for ^{76}Rb(state F: 6.97 MeV) and ^{84}Rb(state E: 2.98 MeV), which should unlikely be observed in experiment. Thus, ^{76}Rb

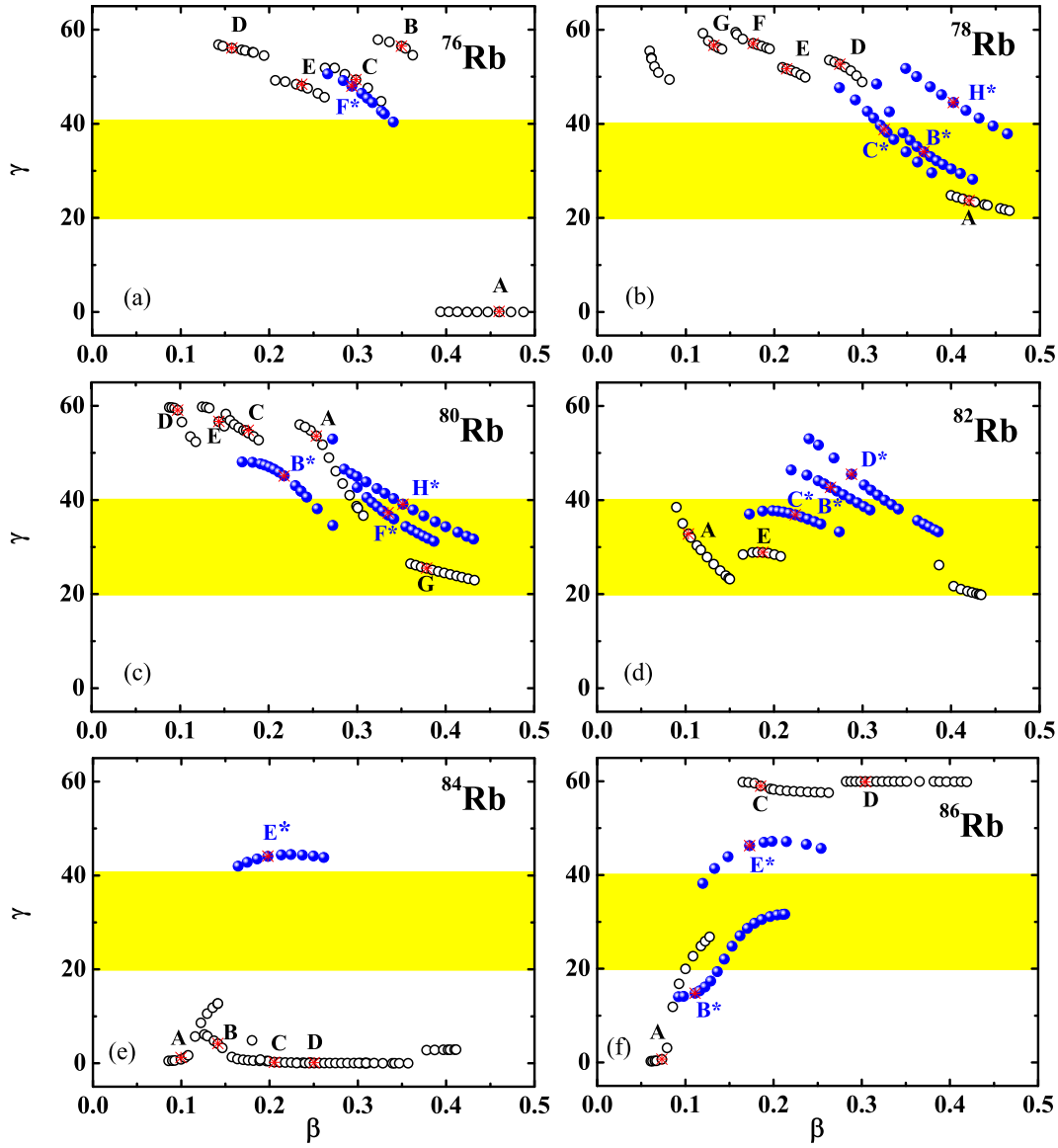

FIG. 2. The triaxiality parameter γ (in degrees) obtained by minimizing the energy is given as a function of the deformation parameter β in triaxial RMF calculations based on the PK1 interaction for ^{76,78,80,82,84,86}Rb. The minima in the energy surfaces for fixed configurations are indicated by stars and are labeled as A, B, C, D, E, F, G, and H. The shaded area represents the triaxiality parameter γ, favorable for nuclear chirality. The suitable states for the appearance of the chirality are marked by solid points with the blue color.

and ^{84}Rb are ruled out from the suggested candidate chiral nuclei.

Apart from the triaxial deformation, the proper particle and hole configuration is also necessary for the appearance of the chiral doublet bands. In Tables I–VI, the calculated total energies $E_{\rm tot}$, triaxial deformation parameters β and γ, corresponding valence nucleon, and unpaired nucleon configurations of the minima are given. The valence nucleon configurations take reference of 40 nucleons which occupy the states below the 50 major shells except for the $g_{9/2}$ subshell. In these tables, the experimental excited energies of different states [52,53,55,60] are shown in comparison with the calculated results. We also show the deformation β_0 of the ground state evaluated in Ref. [69]. As shown in Tables I–VI, the present calculated deformations using the triaxial RMF theory are consistent with those values in Ref. [69] for ^{80,82,84,86}Rb, whereas they are overestimated by about 15% for ^{76,78}Rb. Combining the calculated deformations and configurations, we find the suitable states for the appearance of the chirality, which are marked by the blue color and asterisks in the figures and tables. The possible candidate nuclei of chirality and MχD in odd-odd Rb isotopes are discussed in the following.

For ^{78}Rb, as shown in Table II, the states $B(\beta = 0.37,\ \gamma = 34.0^\circ)$ and $I(\beta = 0.40,\ \gamma = 44.5^\circ)$ have the same unpaired nucleon configuration $\pi g_{9/2}^{1} \otimes \nu g_{9/2}^{-1}$ but have some differences for the valence nucleon configuration. In the previous reported MχD in ^{103}Rh, four $\Delta I = 1$ bands (labeled as 3–6 in Ref. [23]) are based on the identical configuration. Here, it is also

TABLE I. The total energies $E_{\rm tot}$, triaxial deformation parameters β and γ, and their corresponding valence nucleon configurations of minima for states A–F in the configuration-fixed constrained triaxial RMF calculations for ^{76}Rb. The configuration of the valence nucleons takes reference of 40 nucleons which occupy the states below the 50 major shells except for the $g_{9/2}$ subshell. The experimental excited energies E_x(expt.) are shown in comparison with the calculated ones. The data of β_0 are taken from the evaluated values in Ref. [69]. The suitable states for the appearance of the chirality are marked by asterisks with the blue color.

State	Configuration		$E_{\rm tot}$	(β,γ)	E_x(cal.)	E_x(expt.)	β_0
	Valence nucleons	Unpaired nucleons	(MeV)		(MeV)	(MeV)	
A	$\pi(g_{9/2}^3 f_{5/2}^{-2} p_{3/2}^{-2} p_{1/2}^{-2}) \otimes \nu(g_{9/2}^5 f_{5/2}^{-2} p_{3/2}^{-2} p_{1/2}^{-2})$	$\pi g_{9/2}^1 \otimes \nu g_{9/2}^{-1}$	−643.33	(0.46,0.1)	0		0.403
B	$\pi(g_{9/2}^3 f_{5/2}^{-2} p_{3/2}^{-2} p_{1/2}^{-2}) \otimes \nu(g_{9/2}^4 f_{5/2}^{-1} p_{3/2}^{-2} p_{1/2}^{-2})$	$\pi g_{9/2}^1 \otimes \nu f_{5/2}^{-1}$	−642.18	(0.35,56.5)	1.15		
C	$\pi(g_{9/2}^2 f_{5/2}^{-1} p_{3/2}^{-2} p_{1/2}^{-2}) \otimes \nu(g_{9/2}^3 p_{3/2}^{-2} p_{1/2}^{-2})$	$\pi f_{5/2}^{-1} \otimes \nu g_{9/2}^1$	−641.44	(0.30,49.4)			
D	$\pi(p_{3/2}^{-1} p_{1/2}^{-2}) \otimes \nu(g_{9/2}^1 p_{3/2}^{-2})$	$\pi p_{3/2}^{-1} \otimes \nu g_{9/2}^1$	−649.50	(0.16,56.1)			
E	$\pi(g_{9/2}^1 p_{3/2}^{-2} p_{1/2}^{-2}) \otimes \nu(g_{9/2}^2 p_{3/2}^{-1} p_{1/2}^{-2})$	$\pi g_{9/2}^1 \otimes \nu p_{3/2}^{-1}$	−640.41	(0.23,48.4)			
F^*	$\pi(g_{9/2}^1 p_{3/2}^{-3} p_{1/2}^{-2}) \otimes \nu(g_{9/2}^5 f_{5/2}^{-2} p_{3/2}^{-2} p_{1/2}^{-2})$	$\pi g_{9/2}^1 \otimes \nu g_{9/2}^{-1}$	−635.21	(0.30,48.0)	6.97		

TABLE II. Similar to Table I but for ^{78}Rb.

State	Configuration		$E_{\rm tot}$	(β,γ)	E_x(cal.)	E_x(expt.)	β_0
	Valence nucleons	Unpaired nucleons	(MeV)		(MeV)	(MeV)	
A	$\pi(g_{9/2}^4 f_{5/2}^{-4} p_{3/2}^{-2} p_{1/2}^{-1}) \otimes \nu(g_{9/2}^5 p_{3/2}^{-4})$	$\pi p_{1/2}^{-1} \otimes \nu g_{9/2}^{-1}$	−663.93	(0.42,23.7)	0		0.367
B^*	$\pi(g_{9/2}^3 f_{5/2}^{-4} p_{3/2}^{-2}) \otimes \nu(g_{9/2}^5 f_{5/2}^{-2} p_{3/2}^{-2})$	$\pi g_{9/2}^1 \otimes \nu g_{9/2}^{-1}$	−663.67	(0.37,34.0)	0.26	0.115[a]	
C^*	$\pi(g_{9/2}^2 f_{5/2}^{-3} p_{3/2}^{-2}) \otimes \nu(g_{9/2}^5 f_{5/2}^{-2} p_{3/2}^{-2})$	$\pi f_{5/2}^1 \otimes \nu g_{9/2}^{-1}$	−663.42	(0.32,38.8)	0.51	0.111[b]	
D	$\pi(g_{9/2}^2 f_{5/2}^{-3} p_{3/2}^{-2}) \otimes \nu(g_{9/2}^4 f_{5/2}^{-1} p_{3/2}^{-2})$	$\pi f_{5/2}^1 \otimes \nu f_{5/2}^{-1}$	−663.41	(0.27,52.7)			
E	$\pi(g_{9/2}^2 f_{5/2}^{-3} p_{3/2}^{-2}) \otimes \nu(g_{9/2}^3 p_{3/2}^{-2})$	$\pi f_{5/2}^1 \otimes \nu g_{9/2}^1$	−663.34	(0.21,51.7)			
F	$\pi(p_{3/2}^{-1} p_{1/2}^{-2}) \otimes \nu(g_{9/2}^3 p_{1/2}^{-2})$	$\pi p_{3/2}^{-1} \otimes \nu g_{9/2}^1$	−663.26	(0.18,57.1)			
G	$\pi(p_{3/2}^{-1} p_{1/2}^{-2}) \otimes \nu(g_{9/2}^2 p_{1/2}^{-1})$	$\pi p_{3/2}^{-1} \otimes \nu p_{1/2}^{-1}$	−662.30	(0.13,56.7)			
H^*	$\pi(g_{9/2}^3 f_{5/2}^{-4} p_{3/2}^{-2}) \otimes \nu(g_{9/2}^7 f_{5/2}^{-4} p_{3/2}^{-2})$	$\pi g_{9/2}^1 \otimes \nu g_{9/2}^{-1}$	−662.47	(0.40,44.5)	1.46		

[a]The excited energy of state 4^+ taken from Ref. [52].
[b]The excited energy of state 4^- taken from Ref. [52].

TABLE III. Similar to Table I but for ^{80}Rb.

State	Configuration		$E_{\rm tot}$	(β,γ)	E_x(cal.)	E_x(expt.)	β_0
	Valence nucleons	Unpaired nucleons	(MeV)		(MeV)	(MeV)	
A	$\pi(g_{9/2}^2 f_{5/2}^{-1} p_{3/2}^{-2} p_{1/2}^{-2}) \otimes \nu(g_{9/2}^5 p_{1/2}^{-2})$	$\pi f_{5/2}^{-1} \otimes \nu g_{9/2}^{-1}$	−685.64	(0.25,53.6)	0		−0.247
B^*	$\pi(g_{9/2}^1 p_{3/2}^{-2} p_{1/2}^{-2}) \otimes \nu(g_{9/2}^5 p_{1/2}^{-2})$	$\pi g_{9/2}^1 \otimes \nu g_{9/2}^{-1}$	−685.33	(0.22,45.1)	0.31	0.492[a]	
C	$\pi(p_{3/2}^{-1} p_{1/2}^{-2}) \otimes \nu(g_{9/2}^5 p_{1/2}^{-2})$	$\pi p_{3/2}^{-1} \otimes \nu g_{9/2}^{-1}$	−685.01	(0.17,54.8)	0.63	0.398[b]	
D	$\pi(p_{3/2}^{-1} p_{1/2}^{-2}) \otimes \nu g_{9/2}^3$	$\pi p_{3/2}^{-1} \otimes \nu g_{9/2}^1$	−684.69	(0.10,59.1)			
E	$\pi(p_{3/2}^{-1} p_{1/2}^{-2}) \otimes \nu(g_{9/2}^4 p_{1/2}^{-1})$	$\pi p_{3/2}^{-1} \otimes \nu p_{1/2}^{-1}$	−684.67	(0.14,56.7)			
F^*	$\pi(g_{9/2}^3 f_{5/2}^{-2} p_{3/2}^{-4}) \otimes \nu(g_{9/2}^6 p_{3/2}^{-1} p_{1/2}^{-2})$	$\pi g_{9/2}^1 \otimes \nu p_{3/2}^{-1}$	−684.45	(0.33,37.3)	1.19		
G	$\pi(g_{9/2}^4 f_{5/2}^{-3} p_{3/2}^{-2} p_{1/2}^{-2}) \otimes \nu(g_{9/2}^6 p_{3/2}^{-1} p_{1/2}^{-2})$	$\pi f_{5/2}^1 \otimes \nu p_{3/2}^{-1}$	−683.61	(0.38,25.5)			
H^*	$\pi(g_{9/2}^3 p_{3/2}^{-4} p_{1/2}^{-2}) \otimes \nu(g_{9/2}^7 p_{3/2}^{-2} p_{1/2}^{-2})$	$\pi g_{9/2}^1 \otimes \nu g_{9/2}^{-1}$	−683.66	(0.35,39.1)	1.98		

[a]The excited energy of state 6^+ taken from Ref. [53].
[b]The excited energy of state 4^- taken from Ref. [53].

TABLE IV. Similar to Table I but for ^{82}Rb.

State	Configuration		$E_{\rm tot}$	(β,γ)	E_x(cal.)	E_x(expt.)	β_0
	Valence nucleons	Unpaired nucleons	(MeV)		(MeV)	(MeV)	
A	$\pi(p_{3/2}^{-1} p_{1/2}^{-2}) \otimes \nu g_{9/2}^5$	$\pi p_{3/2}^{-1} \otimes \nu g_{9/2}^{-1}$	−706.23	(0.10,32.8)	0		0.086
B^*	$\pi(g_{9/2}^2 p_{3/2}^{-3} p_{1/2}^{-2}) \otimes \nu g_{9/2}^7 p_{1/2}^{-2}$	$\pi p_{3/2}^1 \otimes \nu g_{9/2}^{-1}$	−706.16	(0.26,42.7)	0.07	0.069[a]	
C^*	$\pi(g_{9/2}^1 p_{3/2}^{-2} p_{1/2}^{-2}) \otimes \nu g_{9/2}^7 p_{1/2}^{-2}$	$\pi g_{9/2}^1 \otimes \nu g_{9/2}^{-1}$	−705.99	(0.22,36.9)	0.24	0.301[b]	
D^*	$\pi(g_{9/2}^3 f_{5/2}^{-2} p_{3/2}^{-4}) \otimes \nu g_{9/2}^7 p_{1/2}^{-2}$	$\pi g_{9/2}^1 \otimes \nu g_{9/2}^{-1}$	−705.67	(0.29,45.5)	0.56		
E	$\pi(g_{9/2}^1 p_{3/2}^{-2} p_{1/2}^{-2}) \otimes \nu g_{9/2}^6 p_{1/2}^{-1}$	$\pi g_{9/2}^1 \otimes \nu p_{1/2}^{-1}$	−705.54	(0.19,28.9)			

[a]The excited energy of state 5^- taken from Ref. [55].
[b]The excited energy of state 8^+ taken from Ref. [55].

TABLE V. Similar to Table I but for ^{84}Rb.

State	Configuration		$E_{\rm tot}$	(β,γ)	E_x(cal.)	E_x(expt.)	β_0
	Valence nucleons	Unpaired nucleons	(MeV)		(MeV)	(MeV)	
A	$\pi(p_{3/2}^{-1}p_{1/2}^{-2})\otimes\nu g_{9/2}^{7}$	$\pi p_{3/2}^{-1}\otimes\nu g_{9/2}^{-1}$	−727.39	(0.10,0.1)	0		0.096
B	$\pi(g_{9/2}^{1}p_{3/2}^{-2}p_{1/2}^{-2})\otimes\nu g_{9/2}^{7}$	$\pi g_{9/2}^{1}\otimes\nu g_{9/2}^{-1}$	−726.63	(0.14,4.2)	0.76	0.543[a]	
C	$\pi(g_{9/2}^{2}f_{5/2}^{-1}p_{3/2}^{-2}p_{1/2}^{-2})\otimes\nu g_{9/2}^{7}$	$\pi f_{5/2}^{-1}\otimes\nu g_{9/2}^{-1}$	−725.20	(0.21,0.2)			
D	$\pi(g_{9/2}^{3}f_{5/2}^{-2}p_{3/2}^{-2}p_{1/2}^{-2})\otimes\nu g_{9/2}^{7}$	$\pi g_{9/2}^{1}\otimes\nu g_{9/2}^{-1}$	−724.41	(0.25,0.1)			
E^*	$\pi(g_{9/2}^{1}p_{3/2}^{-2}p_{1/2}^{-2})\otimes\nu g_{9/2}^{9}p_{1/2}^{-2}$	$\pi g_{9/2}^{1}\otimes\nu g_{9/2}^{-1}$	−724.50	(0.21,44.4)	2.89		

[a]The excited energy of state 5^+ taken from Ref. [55].

expected that four $\Delta I=1$ bands based on the $\pi g_{9/2}^{1}\otimes\nu g_{9/2}^{-1}$ configuration (states B and I) as the MχD in ^{78}Rb, whose mechanism is different from those four bands in ^{103}Rh. Besides, the triaxial local minimum $C(\beta=0.32,\gamma=38.8^\circ)$ associates with the $\pi f_{5/2}^{1}\otimes\nu g_{9/2}^{-1}$ configuration, which is a similar configuration with the negative-parity chiral doublet bands in ^{78}Br [25]. Thus, MχDs combined by two sets of positive-parity chiral doublet bands and one set of negative-parity chiral doublet bands are expected to be observed in ^{78}Rb.

As shown in Table III, the triaxial states $B(\beta=0.23,\ \gamma=45.1^\circ)$ and $H(\beta=0.35,\gamma=39.1^\circ)$ in ^{80}Rb, related to the configuration $\pi g_{9/2}^{1}\otimes\nu g_{9/2}^{-1}$, whereas state $F(\beta=0.33,\ \gamma=37.3^\circ)$, related to the $\pi g_{9/2}^{1}\otimes\nu p_{3/2}^{-1}$ configuration, are obtained in the calculated results. Similar with the discussion for ^{78}Rb, the present calculations support the existence of MχD bands combined by two sets of positive-parity chiral doublet bands and one set of negative-parity chiral doublet bands in ^{80}Rb.

In fact, the previously observed doublet bands in ^{78}Rb [52] and ^{80}Rb [53] had shown a hint of chirality. In Fig. 3, we exhibit the observed excited energies of ^{78}Rb and ^{80}Rb for the positive ($\pi=+$) and negative ($\pi=-$) parity bands, in comparison with the reported two sets of chiral doublet bands in ^{78}Br [25]. To show the energy differences between the doublet bands clearly, the excited energies are plotted with a rotor reference subtracted.

On the experimental side, a pair of positive-parity bands (bands 1 and 2) with the $\pi g_{9/2}\otimes\nu g_{9/2}$ configuration linked by the interband transitions had already been reported in ^{78}Rb [52]. As shown in Fig. 3(a), the energy differences between the doublet bands (ΔE) are about 300–500 keV, which is similar to the reported positive-parity chiral doublet bands in ^{78}Rb. Such energy differences ΔE in ^{78}Rb could be interpreted from the chiral vibration mode [15,24,35]. In addition, it should be noted that there are four $\Delta I=1$ negative-parity bands [bands 3–6 shown in Fig. 3(d)] in ^{78}Rb which show mixing between themselves [52]. Their configurations had not been assigned in the previous research. The relationships among these four $\Delta I=1$ bands are very interesting in which chirality might be one of the possible mechanisms. Therefore, finding more linking transitions and extracting the electromagnetic transition probability will be essential to examine the mechanism of these bands including the chirality. The experimental exploration for this nucleus is proceeding in our research group.

The positive-parity band with the $\pi g_{9/2}\otimes\nu g_{9/2}$ configuration had been reported in ^{80}Rb in experiment [53]. As shown in Figs. 3(b) and 3(c), the structure of the positive-parity band in ^{80}Rb is very similar to band 1 in ^{78}Br, including the spin of the bandhead and the energy splitting for an odd-even spin. The present calculated results suggest that the chiral doublet bands may occur based on the $\pi g_{9/2}\otimes\nu g_{9/2}$ configuration, and it is interesting to search for the chiral partner band in the future experiment. The negative-parity bands with the assigned $\pi f_{5/2}\otimes\nu g_{9/2}$ configuration in ^{80}Rb had also been reported [53]. As shown in Fig. 3(e), the first and second negative-parity bands are near degenerate in excited energies (ΔE's are 100–300 keV) before spin $16\hbar$. Such degeneracy is similar to the characteristic of negative-parity chiral doublet bands in ^{78}Br (ΔE's are less than 200 keV for most spins). The negative-parity doublet bands are likely to be the candidate chiral doublet bands based on the properties of the excited energies. However, the observed interband transition between the doublet bands is scarce which is different from the expected properties of chiral doublet bands. Thus, a further experiment is necessary to examine the chirality of ^{80}Rb, and further theoretical studies via the titled axis cranking model or particle rotor model are also necessary.

TABLE VI. Similar to Table I but for ^{86}Rb.

State	Configuration		$E_{\rm tot}$	(β,γ)	E_x(cal.)	E_x(expt.)	β_0
	Valence nucleons	Unpaired nucleons	(MeV)		(MeV)	(MeV)	
A	$\pi(p_{3/2}^{-1}p_{1/2}^{-2})\otimes\nu g_{9/2}^{9}$	$\pi p_{3/2}^{-1}\otimes\nu g_{9/2}^{-1}$	−747.85	(0.07,0.7)	0		0.075
B^*	$\pi(g_{9/2}^{1}p_{3/2}^{-2}p_{1/2}^{-2})\otimes\nu g_{9/2}^{9}$	$\pi g_{9/2}^{1}\otimes\nu g_{9/2}^{-1}$	−746.57	(0.11,14.8)	1.28	1.558[a]	
C	$\pi(g_{9/2}^{2}p_{3/2}^{-3}p_{1/2}^{-2})\otimes\nu g_{9/2}^{10}p_{1/2}^{-1}$	$\pi p_{3/2}^{-1}\otimes\nu p_{1/2}^{-1}$	−743.34	(0.19,59.0)			
D	$\pi(g_{9/2}^{3}f_{5/2}^{-2}p_{3/2}^{-4})\otimes\nu g_{9/2}^{10}g_{7/2}^{1}p_{1/2}^{-2}$	$\pi g_{9/2}^{1}\otimes\nu g_{7/2}^{1}$	−741.68	(0.30,59.9)			
E^*	$\pi(g_{9/2}^{3}f_{5/2}^{-2}p_{3/2}^{-2}p_{1/2}^{-2})\otimes\nu g_{9/2}^{9}$	$\pi g_{9/2}^{1}\otimes\nu g_{9/2}^{-1}$	−741.59	(0.17,46.3)	6.26		

[a]The excited energy of state 7^+ taken from Ref. [60].

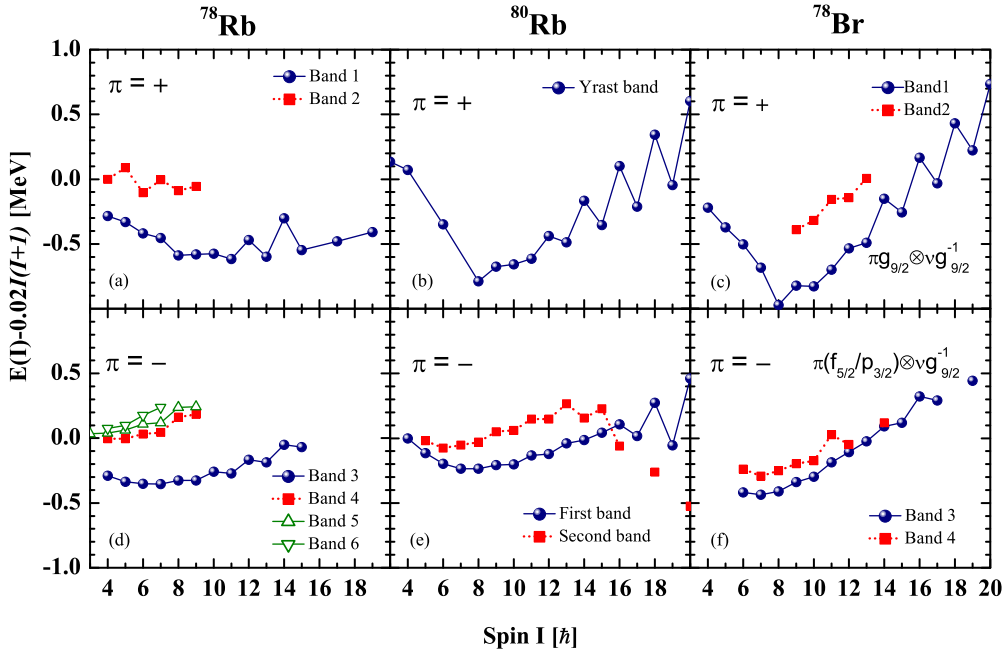

FIG. 3. The observed excited energies $E(I)$ of ^{78}Rb and ^{80}Rb for the positive ($\pi = +$) and negative ($\pi = -$) parity bands, in comparison with two sets of reported chiral doublet bands in ^{78}Br. The data and the name of the bands for ^{78}Rb, ^{80}Rb, and ^{78}Br are taken from Refs. [52,53] and [25], respectively. The excited energies are plotted relative to a rigid-rotor reference. The assigned configurations for the candidate chiral doublet bands in ^{78}Br are listed in the panels.

For ^{82}Rb, the corresponding deformation parameters for the proper proton particle and neutron hole configurations of minima are $B(\beta = 0.26, \gamma = 42.7^\circ)$, $C(\beta = 0.22, \gamma = 36.9^\circ)$, and $D(\beta = 0.29, \gamma = 45.5^\circ)$, respectively. State B corresponds to the $\pi p^1_{3/2} \otimes \nu g^{-1}_{9/2}$ configuration, whereas states C and D associate with the $\pi g^1_{9/2} \otimes \nu g^{-1}_{9/2}$ configurations. Compared with ^{78}Rb and ^{80}Rb, the neutron Fermi surface in ^{82}Rb is closer to the top of the $g_{9/2}$ subshell, which offers the more appropriate particle-hole configuration for chirality. The calculated results support the existence of a MχD phenomenon in ^{82}Rb. As shown in Table IV, the predicted excited energies of the bandhead for the three sets of chiral bands are 0.07, 0.24, and 0.56 MeV, respectively, which should be easily observed in experiment. In fact, a negative-parity band with the $\pi(fp) \otimes \nu g_{9/2}$ configuration and a positive-parity band with the $\pi g_{9/2} \otimes \nu g_{9/2}$ configuration have been observed in Refs. [55,58]. The observed excitation energies of the negative- and positive-parity bandheads are 0.069 and 0.301 MeV [55], which are in good agreement with the calculated results.

For ^{86}Rb, the triaxial deformed state $B(\beta = 0.11, \gamma = 14.8^\circ)$ is obtained with the $\pi g_{9/2} \otimes \nu g_{9/2}$ configuration. Experimentally, a positive-parity band based on the $\pi g_{9/2} \otimes \nu g_{9/2}$ configuration was reported in Ref. [60] with the excited energy of the bandhead 1.56 MeV [60]. The chiral partner band is expected to be observed. The excited state $E(\beta = 0.17, \gamma = 46.3^\circ)$ is also obtained, but it should unlikely be observed in experiment due to the high excited energy of 6.26 MeV.

Considering the above theoretical calculations for the deformations and configurations, ^{78}Rb, ^{80}Rb, and ^{82}Rb should be good candidate chiral nuclei. The previously reported data of ^{78}Rb and ^{80}Rb had shown hints of the chiral doublet bands, which are inconsistent with the present prediction. The predicted best candidate chiral nucleus seems to be ^{82}Rb in which the particle-hole configurations are more appropriate and the excited energies of the triaxial deformation minima are much lower. However, no doublet bands were reported so far. It is highly interesting to search for the chiral doublet bands in ^{82}Rb experimentally.

III. SUMMARY

The chirality in rubidium isotopes is investigated for the first time by using adiabatic and configuration-fixed constrained triaxial RMF theory. Several minima with triaxial deformations and proper particle-hole configurations are obtained in ^{78,80,82,86}Rb where the chiral doublet bands possibly appear. The predicted best candidate chiral nucleus is ^{82}Rb in which no doublet bands were reported so far. It is highly interesting to explore the chirality in ^{82}Rb experimentally. We infer that the previously observed positive-parity doublet bands in ^{78}Rb and negative-parity doublet bands in ^{80}Rb are more likely to be candidate chiral doublet bands. This inference needs to be examined by further experimental studies, such as lifetime measurement.

Furthermore, the possible existence of MχD bands is demonstrated in ^{78,80,82}Rb. We suggest MχD combined by two sets of positive-parity chiral doublet bands and one set of negative-parity chiral doublet bands should be observed in ^{78,80,82}Rb. The present paper will motivate an experimental investigation of these nuclei with the possibility for confirming the predicted MχD in Rb isotopes.

ACKNOWLEDGMENTS

The authors express sincere thanks to Professor J. Meng for his helpful suggestions. This work was partly supported by the National Natural Science Foundation of China (Grants No. 11675094, No. 11622540, and No. 11705102) and the Young Scholars Program of Shandong University, Weihai (Grant No. 2015WHWLJH01).

[1] S. Frauendorf and J. Meng, Nucl. Phys. A **617**, 131 (1997).
[2] K. Starosta, T. Koike, C. J. Chiara, D. B. Fossan, D. R. LaFosse, A. A. Hecht, C. W. Beausang, M. A. Caprio, J. R. Cooper, R. Krücken *et al.*, Phys. Rev. Lett. **86**, 971 (2001).
[3] T. Koike, K. Starosta, C. J. Chiara, D. B. Fossan, and D. R. LaFosse, Phys. Rev. C **63**, 061304(R) (2001).
[4] R. A. Bark, A. M. Baxter, A. P. Byrne, G. D. Dracoulis, T. Kibédi, T. R. McGoram, and S. M. Mullins, Nucl. Phys. A **691**, 577 (2001).
[5] E. Mergel, C. M. Petrache, G. Lo Bianco, H. Hübel, J. Domscheit, D. Roßbach, G. Schönwaßer, N. Nenoff, A. Neuör, and A. Görgen *et al.*, Eur. Phys. J. A **15**, 417 (2002).
[6] T. Koike, K. Starosta, C. J. Chiara, D. B. Fossan, and D. R. LaFosse, Phys. Rev. C **67**, 044319 (2003).
[7] S. Zhu, U. Garg, B. K. Nayak, S. S. Ghugre, N. S. Pattabiraman, D. B. Fossan, T. Koike, K. Starosta, C. Vaman, R. V. F. Janssens *et al.*, Phys. Rev. Lett. **91**, 132501 (2003).
[8] C. Vaman, D. B. Fossan, T. Koike, K. Starosta, I. Y. Lee, and A. O. Macchiavelli, Phys. Rev. Lett. **92**, 032501 (2004).
[9] P. Joshi, D. G. Jenkins, P. M. Raddon, A. J. Simons, R. Wadsworth, A. R. Wilkinson, D. B. Fossan, T. Koike, K. Starosta, C. Vaman *et al.*, Phys. Lett. B **595**, 135 (2004).
[10] J. A. Alcántara-Núñez, J. R. B. Oliveira, E. W. Cybulska, N. H. Medina, M. N. Rao, R. V. Ribas, M. A. Rizzutto, W. A. Seale, F. Falla-Sotelo, K. T. Wiedemann *et al.*, Phys. Rev. C **69**, 024317 (2004).
[11] S. Y. Wang, Y. Z. Liu, T. Komatsubara, Y. J. Ma, and Y. H. Zhang, Phys. Rev. C **74**, 017302 (2006).
[12] E. Grodner, J. Srebrny, A. A. Pasternak, I. Zalewska, T. Morek, C. Droste, J. Mierzejewski, M. Kowalczyk, J. Kownacki, M. Kisieliński *et al.*, Phys. Rev. Lett. **97**, 172501 (2006).
[13] D. Tonev, G. de Angelis, P. Petkov, A. Dewald, S. Brant, S. Frauendorf, D. L. Balabanski, P. Pejovic, D. Bazzacco, P. Bednarczyk *et al.*, Phys. Rev. Lett. **96**, 052501 (2006).
[14] J. Timár, C. Vaman, K. Starosta, D. B. Fossan, T. Koike, D. Sohler, I. Y. Lee, and A. O. Macchiavelli *et al.*, Phys. Rev. C **73**, 011301(R) (2006).
[15] S. Mukhopadhyay, D. Almehed, U. Garg, S. Frauendorf, T. Li, P. V. Madhusudhana Rao, X. Wang, S. S. Ghugre, and M. P. Carpenter, S. Gros *et al.*, Phys. Rev. Lett. **99**, 172501 (2007).
[16] P. Joshi, M. P. Carpenter, D. B. Fossan, T. Koike, E. S. Paul, G. Rainovski, K. Starosta, C. Vaman, and R. Wadsworth, Phys. Rev. Lett. **98**, 102501 (2007).
[17] E. A. Lawrie, P. A. Vymers, J. J. Lawrie, C. Vieu, R. A. Bark, R. Lindsay, G. K. Mabala, S. M. Maliage, P. L. Masiteng, S. M. Mullins *et al.*, Phys. Rev. C **78**, 021305(R) (2008).
[18] T. Suzuki, G. Rainovski, T. Koike, T. Ahn, M. P. Carpenter, A. Costin, M. Danchev, A. Dewald, R. V. F. Janssens, P. Joshi *et al.*, Phys. Rev. C **78**, 031302(R) (2008).
[19] Y. X Zhao, T. Komatsubara, Y. J. Ma, Y. H. Zhang, S. Y. Wang, Y. Z. Liu, and K. Furuno, Chin. Phys. Lett. **26**, 082301 (2009)
[20] P. L. Masiteng, E. A. Lawrie, T. M. Ramashidzha, R. A. Bark, B. G. Carlsson, J. J. Lawrie, R. Lindsay, F. Komati, J. Kau, P. Maine *et al.*, Phys. Lett. B **719**, 83 (2013).
[21] K. Y. Ma, J. B. Lu, Z. Zhang, J. Q. Liu, D. Yang, Y. M. Liu, X. Xu, X. Y. Li, Y. Z. Liu, X. G. Wu *et al.*, Phys. Rev. C **97**, 014305 (2018).
[22] A. D. Ayangeakaa, U. Garg, M. D. Anthony, S. Frauendorf, J. T. Matta, B. K. Nayak, D. Patel, Q. B. Chen, S. Q. Zhang, P. W. Zhao *et al.*, Phys. Rev. Lett. **110**, 172504 (2013).
[23] I. Kuti, Q. B. Chen, J. Timár, D. Sohler, S. Q. Zhang, Z. H. Zhang, P. W. Zhao, J. Meng, K. Starosta, T. Koike *et al.*, Phys. Rev. Lett. **113**, 032501 (2014).
[24] S. Y. Wang, B. Qi, L. Liu, S. Q. Zhang, H. Hua, X. Q. Li, Y. Y. Chen, L. H. Zhu, J. Meng, S. M. Wyngaardt *et al.*, Phys. Lett. B **703**, 40 (2011).
[25] C. Liu, S. Y. Wang, R. A. Bark, S. Q. Zhang, J. Meng, B. Qi, P. Jones, S. M. Wyngaardt, J. Zhao, C. Xu *et al.*, Phys. Rev. Lett. **116**, 112501 (2016).
[26] J. Meng, B. Qi, S. Q. Zhang, and S. Y. Wang, Mod. Phys. Lett. A **23**, 2560 (2008).
[27] V. I. Dimitrov, S. Frauendorf, and F. Dönau, Phys. Rev. Lett. **84**, 5732 (2000).
[28] P. Olbratowski, J. Dobaczewski, J. Dudek, and W. Plóciennik, Phys. Rev. Lett. **93**, 052501 (2004).
[29] P. Olbratowski, J. Dobaczewski, and J. Dudek, Phys. Rev. C **73**, 054308 (2006).
[30] J. Peng, J. Meng, and S. Q. Zhang, Phys. Rev. C **68**, 044324 (2003).
[31] T. Koike, K. Starosta, and I. Hamamoto, Phys. Rev. Lett. **93**, 172502 (2004).
[32] S. Q. Zhang, B. Qi, S. Y. Wang, and J. Meng, Phys. Rev. C **75**, 044307 (2007).
[33] S. Y. Wang, S. Q. Zhang, B. Qi, and J. Meng, Phys. Rev. C **75**, 024309 (2007).
[34] S. Y. Wang, S. Q. Zhang, B. Qi, J. Peng, J. M. Yao, and J. Meng, Phys. Rev. C **77**, 034314 (2008).
[35] B. Qi, S. Q. Zhang, J. Meng, and S. Frauendorf, Phys. Lett. B **675**, 175 (2009).
[36] B. Qi, S. Q. Zhang, S. Y. Wang, J. M. Yao, and J. Meng, Phys. Rev. C **79**, 041302(R) (2009).
[37] S. Y. Wang, B. Qi, and D. P. Sun, Phys. Rev. C **82**, 027303 (2010).
[38] E. A. Lawrie and O. Shirinda, Phys. Lett. B **689**, 66 (2010).
[39] B. Qi, S. Q. Zhang, S. Y. Wang, J. Meng, and T. Koike, Phys. Rev. C **83**, 034303 (2011).
[40] O. Shirinda and E. A. Lawrie, Eur. Phys. J. A **48**, 118 (2012).
[41] H. Jia, B. Qi, S. Y. Wang, S. Wang, and C. Liu, Chin. Phys. C **40**, 124103 (2016).
[42] S. Brant, D. Vretenar, and A. Ventura, Phys. Rev. C **69**, 017304 (2004).
[43] D. Tonev, G. de Angelis, S. Brant, S. Frauendorf, P. Petkov, A. Dewald, F. Dönau, D. L. Balabanski, Q. Zhong, P. Pejovicet *et al.*, Phys. Rev. C **76**, 044313 (2007).
[44] S. Brant and C. M. Petrache, Phys. Rev. C **79**, 054326 (2009).
[45] H. G. Ganev and S. Brant, Phys. Rev. C **82**, 034328 (2010).

[46] Q. B. Chen, S. Q. Zhang, P. W. Zhao, R. V. Jolos, and J. Meng, Phys. Rev. C **87**, 024314 (2013).
[47] Q. B. Chen, S. Q. Zhang, P. W. Zhao, R. V. Jolos, and J. Meng, Phys. Rev. C **94**, 044301 (2016).
[48] J. Meng and S. Q. Zhang, J. Phys. G: Nucl. Part. Phys. **37**, 064025 (2010).
[49] J. Meng, J. Peng, S. Q. Zhang, and S. G. Zhou, Phys. Rev. C **73**, 037303 (2006).
[50] A. Harder, M. K. Kabadiyski, K. P. Lieb, D. Rudolph, C. J. Gross, R. A. Cunningham, F. Hannachi, J. Simpson, D. D. Warner, H. A. Roth *et al.*, Phys. Rev. C **51**, 2932 (1995).
[51] A. Harder, A. Jungclaus, M. K. Kabadiyski, D. Kast, K. P. Lieb, D. Rudolph, M. Weiszflog, T. D. Johnson, G. Winter, C. J. Gross *et al.*, Phys. Rev. C **55**, 1680 (1997).
[52] R. A. Kaye, J. Döring, J. W. Holcomb, G. D. Johns, T. D. Johnson, M. A. Riley, G. N. Sylvan, P. C. Womble, V. A. Wood, S. L. Tabor *et al.*, Phys. Rev. C **54**, 1038 (1996).
[53] C. Y. He, S. F. Shen, S. X. Wen, L. H. Zhu, X. G. Wu, G. S. Li, Y. Zhao, Y. P. Yan, Z. J. Bai, Y. C. Wu *et al.*, Phys. Rev. C **87**, 034320 (2013).
[54] J. Döring, R. Schwengner, L. Funke, H. Rotter, G. Winter, B. Cederwall, F. Lidén, A. Johnson, A. Atac, J. Nyberg *et al.*, Phys. Rev. C **50**, 1845 (1994).
[55] R. Schwengner, G. Rainovski, H. Schnare, A. Wagner, F. Dönau, A. Jungclaus, M. Hausmann, O. Iordanov, K. P. Lieb, D. R. Napoli *et al.*, Phys. Rev. C **66**, 024310 (2002).
[56] J. Döring, G. D. Johns, R. A. Kaye, M. A. Riley, and S. L. Tabor, Phys. Rev. C **60**, 014314 (1999).
[57] R. Schwengner, G. Rainovski, H. Schnare, A. Wagner, S. Frauendorf, F. Dönau, A. Jungclaus, M. Hausmann, O. Yordanov, K. P. Lieb *et al.*, Phys. Rev. C **80**, 044305 (2009).
[58] S. F. Shen, G. B. Han, S. X. Wen, F. Pan, J. Y. Zhu, J. Z. Gu, J. P. Draayer, X. G. Wu, L. H Zhu, C. Y. He *et al.*, Phys. Rev. C **82**, 014306 (2010).
[59] R. Schwengner, G. Winter, J. Reif, H. Prade, L. Käubler, R. Wirowski, N. Nicolay, S. Albers, S. Efsber, P. von Brentano *et al.*, Nucl. Phys. A **584**, 159 (1995).
[60] G. Winter, R. Schwengner, J. Reif, H. Prade, J. Döring, R. Wirowski, N. Nicolay, P. von Brentano, H. Grawe, and R. Schubart, Phys. Rev. C **49**, 2427 (1994).
[61] J. M. Yao, B. Qi, S. Q. Zhang, J. Peng, S. Y. Wang, and J. Meng, Phys. Rev. C **79**, 067302 (2009).
[62] J. Peng, H. Sagawa, S. Q. Zhang, J. M. Yao, Y. Zhang, and J. Meng, Phys. Rev. C **77**, 024309 (2008).
[63] J. Li, S. Q. Zhang, and J. Meng, Phys. Rev. C **83**, 037301 (2011).
[64] B. Qi, H. Jia, N. B. Zhang, C. Liu, and S. Y. Wang, Phys. Rev. C **88**, 027302 (2013).
[65] J. Li, Phys. Rev. C **97**, 034306 (2018).
[66] W. H. Long, J. Meng, N. Van Giai, and S. G. Zhou, Phys. Rev. C **69**, 034319 (2004).
[67] G. A. Lalazissis, J. König, and P. Ring, Phys. Rev. C **55**, 540 (1997).
[68] Y. Sugahara and H. Toki, Nucl. Phys. A **579**, 557 (1994).
[69] P. Möller, J. R. Nix, W. D. Myers, and W. J. Swiatecki, At. Data Nucl. Data Tables **109**, 1 (2016).